REVIEW OF SCIENTIFIC INSTRUMENTS **87**, 075110 (2016)

Superconducting radio-frequency resonator in magnetic fields up to 6 T

M. S. Ebrahimi,[1,2] N. Stallkamp,[1,3] W. Quint,[1,2] M. Wiesel,[1,2,4] M. Vogel,[1] A. Martin,[4] and G. Birkl[4]
[1]*GSI Helmholtzzentrum für Schwerionenforschung, 64291 Darmstadt, Germany*
[2]*Physikalisches Institut, Ruprecht Karls-Universität, 69120 Heidelberg, Germany*
[3]*Helmholtz-Institut Jena, 07743 Jena, Germany*
[4]*Institut für Angewandte Physik, TU Darmstadt, 64291 Darmstadt, Germany*

(Received 25 February 2016; accepted 28 June 2016; published online 18 July 2016)

We have measured the characteristics of a superconducting radio-frequency resonator in an external magnetic field. The magnetic field strength has been varied with 10 mT resolution between zero and 6 T. The resonance frequency and the quality factor of the resonator have been found to change significantly as a function of the magnetic field strength. Both parameters show a hysteresis effect which is more pronounced for the resonance frequency. Quantitative knowledge of such behaviour is particularly important when experiments require specific values of resonance frequency and quality factor or when the magnetic field is changed while the resonator is in the superconducting state. *Published by AIP Publishing.* [http://dx.doi.org/10.1063/1.4958647]

I. INTRODUCTION

Many detection schemes for electronic signals rely on resonant detection. High quality factors allow signal amplification in the relevant frequency range by many orders of magnitude. Ion trap experiments commonly employ resonance circuits in the radio-frequency domain for pick-up of signals created by the oscillating charges in the trap, usually to the end of measuring the oscillation frequencies or cooling the ion motion.[1,2] Since the currents induced by the ion motion are typically small (in the range of femto-ampere to pico-ampere), a resonant circuit is used to increase the detected voltage which corresponds to that current, since in resonance, it represents an elevated resistance. The voltage signal is usually further amplified and then measured, and its Fourier analysis yields the oscillation frequency spectrum of the charged particles in the trap.[3] In principle, the resonance frequency and quality factor of a resonator can be calculated from the chosen geometry and material properties, however, not to high precision. This is mainly due to the influence of geometric details on the inductance and capacitance, and is particularly true when the resonator is superconducting, operated in high magnetic field, and used to detect radio frequency signals, as will be discussed below. For application in a given experiment, resonance frequency and quality factor usually need to be chosen specifically. However, as the resonator characteristics are found to depend not only on intrinsic properties but also on experimental parameters such as temperature and in particular magnetic field strength, it is valuable to have quantitative information on these dependences. In this study, we systematically investigate the properties of a superconducting resonator in the presence of a magnetic field of up to 6 T strength with a resolution of 10 mT, thus significantly extending previous measurements[4] into the field strength domain most common for ion trap experiments.

II. SETUP

A. Resonator

A generic resonance circuit is constituted by the total inductance L of the resonator and the total capacity C of it and its wiring. It is resonant at a frequency $\omega_0 = 1/\sqrt{LC}$ and in resonance represents an Ohmic resistance of $R_p = \omega_0 L Q$, where the quality factor Q is the ratio of the total energy in the circuit and the resistive energy loss per radian. Typical values of Q range from a few hundred to a few hundreds of thousands.[4–6] In many applications, the quality factor and the resonance resistance are desired to be as high as possible, requiring C to be small, which is non-trivial for high parasitic capacitances within the setup. Most often, the potentially high quality factor is the motivation to prefer superconducting rf-resonators over normal conducting ones.

The present superconducting resonator mainly consists of a coil made from niobium-titanium (NbTi, a type-II superconductor) wire wound on a polytetrafluoroethylene (PTFE) core and sealed in a cylindrical oxygen-free high-conductivity copper (OFHC) housing. In a field-free configuration, the NbTi becomes superconducting below $T_c = 9.2$ K and has an upper critical field strength B_{c2} of about 14.5 T at zero temperature.[7,8] This makes the use of NbTi in high magnetic field experiments advantageous over other superconductor materials, such as, pure niobium, tantalum, or lead, since generally, the upper critical field strength of type-II superconductors exceeds the critical field strength of type-I superconductors significantly.[9] Type-I superconductors below their critical field strength and type-II superconductors below their lower critical field strength B_{c1} are in the so-called "Meissner phase," i.e., they exclude an external magnetic field. A type-II-superconductor in an external field between the lower critical field strength B_{c1} and the upper critical field strength B_{c2} is in the so-called "Shubnikov phase," i.e., it is pervaded by the magnetic field in quanta of the magnetic flux $\Phi_0 = h/(2e) \approx 2.067 \cdot 10^{-15}\,\mathrm{Tm}^2$, which create vortices in the superconductor. These are circular super-currents around normal-conducting cores which form about the magnetic field lines.[8] The local inhomogeneities in the lattice structure of the superconducting material lead to a localization of vortices, which is commonly known as vortex pinning.[9] In the presence of an ac-current such as the present radio-frequency signal, the interaction of the vortices with the current gives rise to an effective resistance which leads to signal loss. This means that the energy loss per oscillation is non-zero even for such a superconductor, as has been detailed for example in Ref. 9. The loss scales with the third power of the frequency, such that the use of a type-II superconducting resonator is advantageous over a normal-conducting resonator only for sufficiently small frequencies, typically on the scale of few tens of MHz and below, which however includes most of the range of ion oscillation frequencies common to ion trap experiments.

The resonator coil tested here is of toroidal geometry, i.e., the wire is wound around a toroidal PTFE core, see Figure 1. The cross section of this toroid is rectangular with slightly rounded edges, the inner and outer diameters d_1 and d_2 being 23 mm and 38 mm, respectively, and a toroid thickness a of 22 mm. The design of the resonator is based on the resonators developed by the BASE experiment at CERN.[10] The wire is made of a NbTi conductor with a diameter δ of 0.075 mm and a perfluoroalkoxy (PFA) insulation. The diameter is larger (by at least two orders of magnitude) than the London penetration depth and the expected coherence length in the material, such that size effects are not expected.[11] Each of the 16 sections on the toroidal core (see Figure 1) has 3 layers of 15–20 windings, making up a total wire length of 48 m, including the leads between sections. Between each wire layer there is one layer of PTFE tape to further fix the winding geometry. The separation of the sections in Figure 1 is exaggerated for better visibility and will be ignored in the upcoming estimations. The

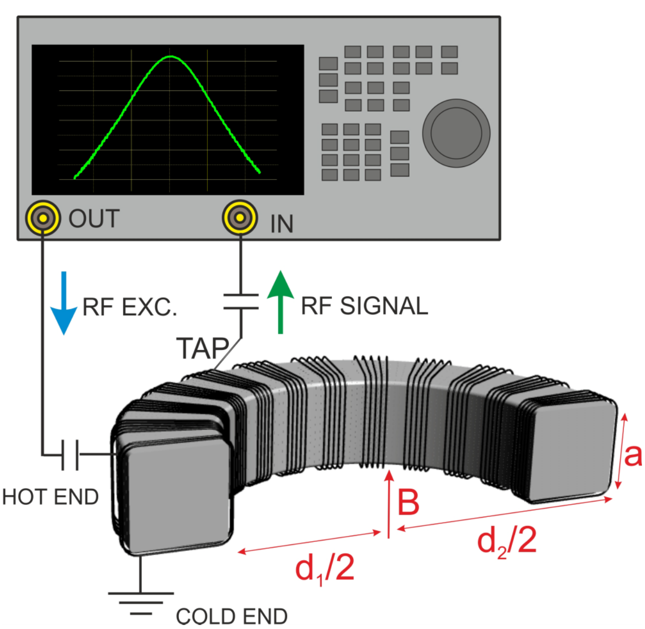

FIG. 1. Schematic of the toroidal superconducting resonator connected to a spectrum analyzer. The resonator housing is omitted and the torus is cut in half for better representation.

inductance L_c of a toroidal coil with rectangular cross section can be approximated by[12]

$$L_c \approx \kappa N^2 a \ln\left(\frac{d_2}{d_1}\right), \tag{1}$$

where $\kappa = 0.46 \cdot 10^{-6}$ H/m is a geometry-specific factor[12] and N is the total winding number, taken to be $N = 800$. This results in $L_c \approx 3$ mH. The coil inductance L_c constitutes the dominant part of the total resonator inductance L, apart from a reduction[12] by the presence of the OFHC resonator housing with 48 mm diameter and 40 mm height, estimated to result in $L \approx 2.4$ mH.

The self-capacitance C_c of such a coil can be approximated by[13]

$$C_c \approx \chi \epsilon_0 l \left(\frac{\epsilon_r \theta}{\ln \frac{d_w}{d_2}} + \cot \frac{\theta}{2} - 1 \right), \tag{2}$$

where $l \approx (d_2 - d_1) + 2a$ is the average single-turn conductor length, $\theta = \arccos(1 - \epsilon_r^{-1} \ln(d_w/d_2))$ accounts for the effective diameter $d_w \approx 42$ mm of the core including the winding, $\epsilon_0 = 8.85 \cdot 10^{-12}$ F/m and $\epsilon_r = 2.1$ are the permittivity of free space and the relative permittivity of the insulator, respectively, and $\chi \approx 1.366$ again is a geometry factor.[13] For the present arrangement, this results in $C_c \approx 8$ pF. The total capacitance C of the resonance circuit consists of the self-capacitance C_c of the coil, and the parasitic capacitances of the coil-housing arrangement and the wiring. This amounts to $C \approx 10$ pF, together with $L \approx 2.4$ mH leading to a resonance frequency of $\omega_0 \approx 2\pi \cdot 1$ MHz. A measurement of the zero-field resonator properties at 4 K yields $R_p \approx 601$ MΩ and a quality factor of $Q = 371\,19$ at a resonance frequency of $\omega_0 = 2\pi \cdot 101\,929\,1$ Hz. It leads to corresponding values of $L = R_p/(\omega_0 Q) = 2.53$ mH and $C = Q/(\omega_0 R_p) = 9.64$ pF, which are in fair agreement with the calculated values above.

B. Magnet setup

The measurements have been performed with the resonator center located at the center of the homogeneous magnetic field of a superconducting magnet, as shown in Figure 2. The central axes of the magnetic field, of the housing cylinder, and of the toroid are identical. The central field strength can be varied continuously between zero and 6 T. The resonator is cooled to achieve the superconducting state by a pulse tube cooler which is the central part of the cryostat inserted into the warm bore of the magnet. It has a cooling power of 1 W at 4 K for the central stage, and a surrounding stage with 40 W cooling power at 45 K, which acts as a thermal shield to protect the 4 K stage from room temperature radiation. The magnet bore is evacuated by a turbo-molecular pump to obtain isolation vacuum. The temperatures of the two stages and of the resonator housing are measured by temperature sensors. The resonator is excited by the rf output of a Rigol DSA-815TG tracking spectrum analyzer, and the response is recorded as indicated in the schematic shown in Figure 1. The so-called "cold end" of the coil is grounded at the 4 K stage, while the "hot end" is used for rf-excitation by the spectrum

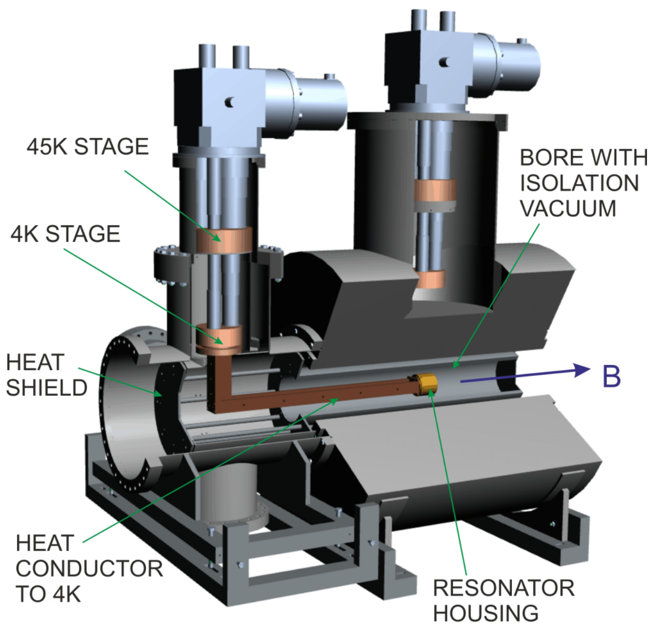

FIG. 2. Schematic overview of the measurement apparatus. The superconducting magnet and heat shields have been cut open for better representation.

analyzer. The response of the system is measured by detection of the signal as obtained from the "tap," which is an electrical connection attached to the coil between its ends. Both signals (excitation and response) are coupled capacitively through air to the hot end and analyzer, respectively, by bringing the ends of the respective conductors in close parallel proximity. For measurements without excitation, the readout is done directly through a small capacitance.

III. MEASUREMENTS

The resonator response measurements have been performed with the resonator being brought into the superconducting state prior to introduction of the magnetic field ("zero-field cooling"). This situation is to be distinguished from the reverse order ("field cooling") as the field penetration of the superconductor behaves differently, as discussed in Refs. 8 and 9.

A. Spectral response

We have measured the spectral response of the resonator circuit upon tracking excitation for values of the magnetic field strength between zero and 6 T with a resolution of 10 mT. Figure 3 shows response curves (signal strength as a function of frequency) for 16 selected values of the magnetic field strength in an upward scan of the B-field. Obviously, there is a significant change in the spectral response with respect to the resonance frequency, the signal width (i.e., the quality factor), and the overall magnitude of the signal.

B. Resonance frequency

Figure 4 shows the resonance frequency as a function of the magnetic field strength for all resonance curves of

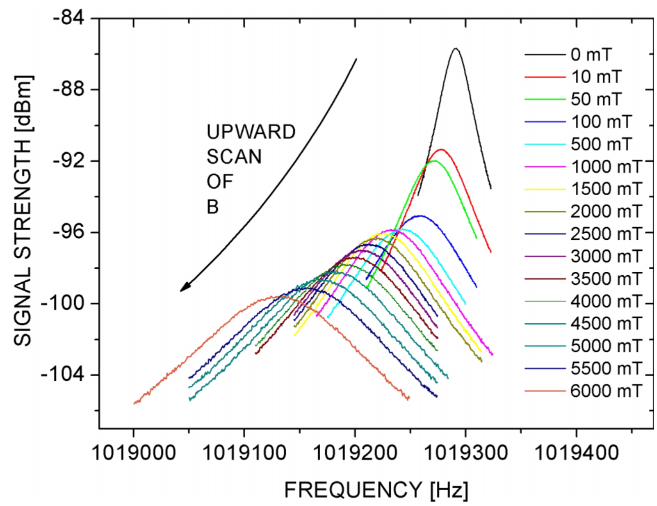

FIG. 3. Measured resonator response as a function of the frequency for selected values of the magnetic field strength.

the upward scan. The overall trend is for the resonance frequency to decrease monotonically with increasing magnetic field strength, particularly strongly between the smallest field values. The inset of Figure 4 shows an initial steep decrease from the field-free case to the point at 10 mT and a relative flattening of the curve at about 120 mT. Overall, the resonance frequency decreases from 101 929 0 Hz in the field-free case to 101 912 9 Hz at $B = 6$ T, which is a relative change of $1.5 \cdot 10^{-4}$.

C. Quality factor

With increasing magnetic field, the quality factor $Q(B)$ decreases, as seen by the broadening of the resonance. To obtain the quality factor, the measured resonance curve is fitted with a Lorentz function, and the ratio of the resonance frequency and the FWHM of the curve defines $Q(B)$. The hence measured value may somewhat underestimate the real quality factor due to the finite bandwidth β, but this is expected

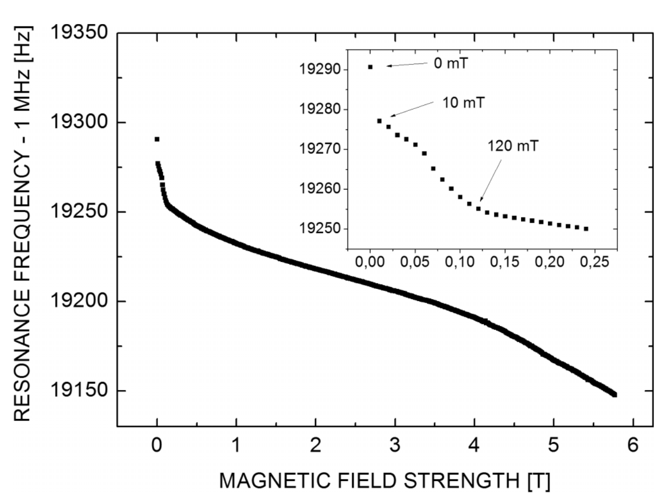

FIG. 4. Measured resonance frequency as a function of the magnetic field strength. Error bars are much smaller than the symbols. Inset: The first 25 data points.

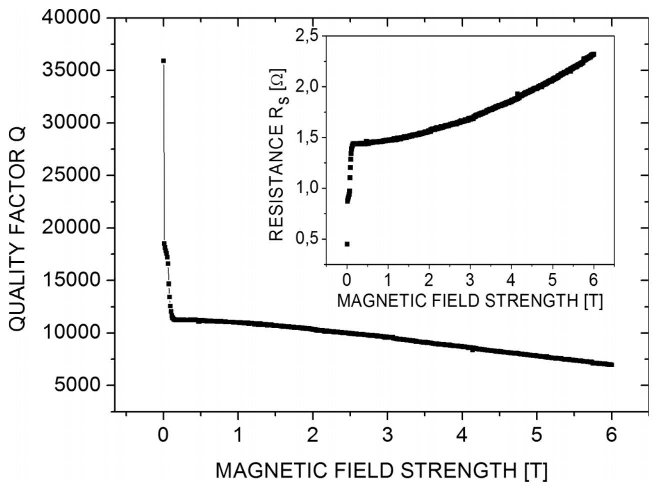

FIG. 5. Measured quality factor Q as a function of the magnetic field strength. Error bars are smaller than the symbols. Inset: Calculated resistance R_s.

to be relevant only for the highest values of $Q(B)$. Figure 5 shows the resulting quality factor as a function of the magnetic field strength. The value of $Q(B)$ decreases by a factor of about 3.5 within the initial 120 mT, and then slowly decreases further. This effect is much stronger than the one observed in Ref. 4, where the quality factor only changes by about -15% between 0 and 1 T.

D. Discussion

One expects a resonance frequency shift due to resistive loss in the superconductor resulting from the interaction of the ac current at frequency ω with vortices of the magnetic field.[9] The onset of resistive loss should occur at about the transition between the Meissner and the Shubnikov phase, i.e., at about the lower critical field strength of the superconductor. The value of B_{c1} of NbTi at $T = 0$ K is about 22 mT.[17] According to[9]

$$B_{c1}(T) = B_{c1}(T=0)\left(1 - \frac{T^2}{T_c^2}\right), \tag{3}$$

the value of B_{c1} at 4.2 K is about 18 mT (in fair concurrence with 12.4 mT given in Ref. 18 and 14 mT given in Ref. 19).

The loss is expected to be given by a convolution of the spatial current density distribution $j(r)$ in the superconductor with the spatial distribution of vortices $\sigma(r)$ as a function of the magnetic field strength. To be more precise, the resistive loss $\epsilon(r)$ of energy is given by $\epsilon(r) \propto j^2(r)\sigma(r)$, see the discussion in Ref. 14. It is, however, extremely difficult to calculate the loss in this manner due to our insufficient knowledge of the involved quantities.

Under the assumption that resistive loss is the only mechanism that shifts the resonance frequency, the observed shift of ω_0 (Figure 4) can be used to calculate the corresponding damping according to $\omega_0^2(B=0) - \omega_0^2(B) = \eta^2(B)$ with the damping term $\eta(B) = R_s(B)/(2L)$, where $R_s(B)$ represents the resulting series Ohmic resistance causing the loss. This would imply R_s is of the order of hundreds of ohms. According to $Q = \omega_0 L/R_s$, this would lead to quality factors lower than the observed ones by about two orders of magnitude. Hence, the observed resonance frequency shift cannot be simply explained by resistive loss. This is also obvious from the inset of Figure 5, where the series resistance $R_s = \omega_0 L/Q$ resulting from the measured quality factor Q is plotted, amounting to few ohms only, which is what can be expected from such a resonator.

Both the dependences of the resonance frequency and of the quality factor on the magnetic field strength show an initial strong decrease and a characteristic flattening at about B =120 mT. Since the observed shift of the resonance frequency cannot be explained by resistive loss alone, it is plausible to assume a field-dependent increase of the resonator's capacitance (and possibly also inductance), which could explain both behaviours. In particular, the capacitance is very sensitive to changes of the coil geometry, as can be seen from Equation (2) (see also the discussion in Ref. 13). When looking at the change of resonator capacity resulting from a change of the effective coil diameter d_w,

$$\frac{\partial C_c}{\partial d_w} = \chi\epsilon_0\epsilon_r l \frac{1}{d_w}\ln^{-2}\left(\frac{d_w}{d_2}\right)\arccos\left(1 - \frac{1}{\epsilon_r}\ln\left(\frac{d_w}{d_2}\right)\right), \tag{4}$$

then for the present resonator it will amount to 1.1 pF/mm (which is a stronger relative change than that of the inductance, by one order of magnitude), such that a relative change of the capacity by 10^{-4} can easily result from variation of the effective coil diameter on the micrometre scale. Such a variation may well be caused by magnetic forces on the resonator due to temporal and/or spatial field gradients. This indicates that in the manufacturing of such resonators, special care has to be taken to make the winding structure insensitive to external influence, in particular when they are subjected to large magnetic field changes.

E. Hysteresis

When the magnetic field is increased from zero and then decreased to zero again, the resonance frequency and the quality factor show a hysteresis effect, as has previously been observed in the microwave frequency regime for much smaller values of the applied magnetic field.[14,15] In our work, investigating an extended range from zero to 6 T, we find a pronounced hysteresis for the resonance frequency within the full range of the magnetic field scan, see Figure 6. In contrast, the quality factor shows no significant hysteresis except for the zero-field value, see Figure 7. This corroborates the statement that the observed shift of the resonance frequency is not due to resistive loss alone. Figure 6 compares the measured resonance frequencies for an upward and downward scan of the magnetic field. The resonance frequencies of the downward scan stay significantly below the upward scan values, with relative differences of up to about 10^{-4}. In total, five such cycles have been measured, of which cycle number 1 is shown in the figure. The cycle begins in the "virgin state" at zero magnetic field indicated by (1), the field is scanned up to 6 T (2), where the downscan begins (3), and ends at zero field (4). When this is repeated, the resonance frequency at all four points is shifted down with each scan, as indicated in the inset of the figure. It shows the resonance

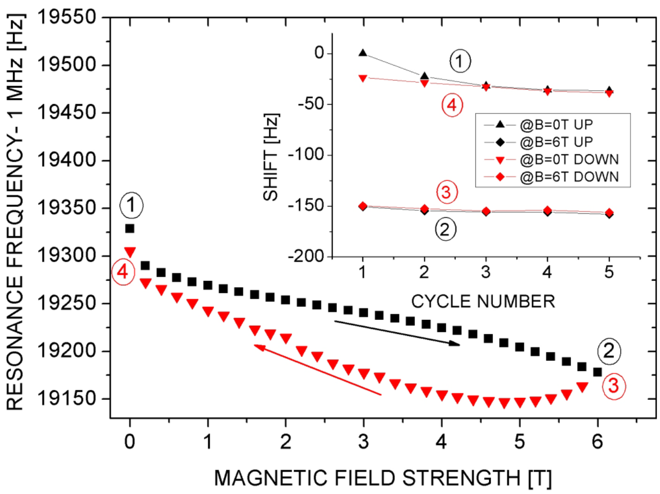

FIG. 6. Measured resonance frequency ω_0 as a function of the magnetic field strength for an up-scan followed by a down-scan of the field. Full squares: Upward scan, full triangles: downward scan. The inset is explained in the text.

frequency relative to the initial frequency, i.e., point (1) of the first cycle, as a function of the cycle number. The initial difference between (1) and (4) of about −25 Hz vanishes with increasing cycle number, however, the cycles tend to lower the overall frequencies, as seen by the negative slope of the curves in the inset. A hysteresis phenomenon is expected to be caused by the dynamics of the vortex distribution in the changing external field.[9] A vortex-free state is not achieved after a cycle of magnetic field sweep (the material does not "recover"), therefore the quality factors and resonance frequencies do not match their initial zero-magnetic-field values after the full scan. The observed differences between the states (1) and (4) in Figures 6 and 7 may in part be attributed to this effect, although it may also be mimicked by field-dependent geometry changes. The occurrence of such "remanent" vortices in type-II superconductors has been discussed in Ref. 16 as part of the irreversible processes in superconductors. The loss-free virgin state is only recovered

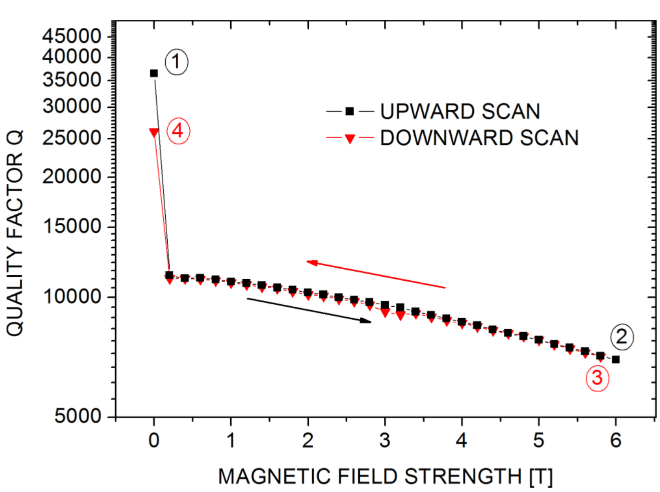

FIG. 7. Measured quality factor Q as a function of the magnetic field strength for the first full scan starting from the virgin state. Full squares: upward scan, full triangles: downward scan.

when the resonator is brought out of the superconducting state.

IV. CONCLUSION

We have measured the resonance frequency and quality factor of a superconducting radio-frequency resonator in an external magnetic field between zero and 6 T in steps of 10 mT. While in this work we have investigated a resonator of toroidal geometry, it is expected from the underlying physics that the findings qualitatively hold true also for other geometries, such as solenoids and coplanar resonators. Both the resonance frequency and quality factor are found to decrease with increasing magnetic field strength. A likely mechanism for the reduction in resonance frequency is the presence of field-dependent forces which effectively change the resonator capacitance. While additional contributions might arise from loss mechanisms due to the interaction of the rf current with the vortices in the superconductor in the presence of the external magnetic field, the observed shift of the resonance frequency exceeds the effect on the quality factor, such that this effect can only explain a minor contribution.

When the magnetic field is scanned up and down, both the resonance frequency and quality factor show a hysteresis effect, in a way such that the values never recover to their initial state after each full scanning cycle. While the hysteresis is pronounced for the resonance frequency within the full scan range, it is insignificant for the quality factor apart from the zero-field value. The obtained results present important input parameters when designing and operating superconducting resonators, particularly in strong magnetic fields, as common to many ion trap experiments.

ACKNOWLEDGMENTS

We gratefully acknowledge the help of the BASE team at CERN in the manufacturing of the resonator. M.S.E. is grateful for the positive reception and support he received during his academic visit to BASE, in particular we wish to thank Matthias Borchert for his sustained involvement. This work received partial financial support from DFG under the Grant No. BI 647/4-1 and from HIC for FAIR.

[1] W. M. Itano, J. C. Bergquist, J. J. Bollinger, and D. J. Wineland, "Cooling methods in ion traps," Phys. Scr. **T59**, 106 (1995).
[2] G. Werth, V. N. Gheorghe, and F. G. Major, *Charged Particle Traps* (Springer, Heidelberg, 2005).
[3] A. G. Marshall, C. L. Hendrickson, and G. S. Jackson, "Fourier transform ion cyclotron resonance mass spectrometry: A primer," Mass Spectrom. Rev. **17**, 135 (1998).
[4] S. Ulmer *et al.*, "The quality factor of a superconducting rf resonator in a magnetic field," Rev. Sci. Instrum. **80**, 123302 (2009).
[5] H. Häffner *et al.*, "Double penning trap technique for precise g factor determinations in highly charged ions," Eur. Phys. J. D **22**, 163 (2003).
[6] M. Bonaldi *et al.*, "High-Q tunable LC-resonator operating at cryogenic temperature," Rev. Sci. Instrum. **69**, 3690 (1998).
[7] A. Godeke, "Limits of NbTi and Nb_3 Sn and development of W&R Bi-2212 high field accelerator magnets," IEEE Trans. Appl. Supercond. **17**, 1149 (2007).
[8] A. V. Narlikar, *Superconductors* (Oxford University Press, 2014).

[9]M. Tinkham, *Introduction to Superconductivity* (Dover Publications, Mineola, 2004).
[10]C. Smorra *et al.*, "BASE—The Baryon Antibaryon Symmetry Experiment," Eur. Phys. J.: Spec. Top. **224**, 3055 (2015).
[11]P. A. Venegas and E. Sardella, "Vortex lattice and matching fields for a long superconducting wire," Phys. Rev. B **58**, 5789 (1998).
[12]F. Terman, *Radio Engineers' Handbook* (McGraw-Hill, 1943).
[13]S. W. Pasko, M. K. Kazimierczuk, and B. Grzesik, "Self-capacitance of coupled toroidal inductors for EMI filters," IEEE Trans. Electromagn. Compat. **57**, 216 (2015).
[14]D. Bothner *et al.*, "Magnetic hysteresis effects in superconducting coplanar microwave resonators," Phys. Rev. B **86**, 014517 (2012).
[15]C. P. Bean, "Magnetization of hard superconductors," Phys. Rev. Lett. **8**, 250 (1962).
[16]C. P. Poole, Jr. *et al.*, *Superconductivity*, 2nd ed. (Elsevier, 2007).
[17]Given as about 225 Oe for the 50/50 alloy Nb/Ti in M. N. Kunchur and S. J. Poon, "Critical fields and critical currents of superconducting disks in transverse magnetic fields," Phys. Rev. B **43**, 2916 (1991).
[18]K. R. Krebs, J. Pytlik, and E. Seibt, Magnetisierungsmessungen an NbTi-, NbZr-, Nb_3Sn- und V_3Ga-Materialien bei 4,2 K, Institut für Experimentelle Kernphysik, Kernforschungszentrum Karlsruhe, KFK-1683, 1972.
[19]M. A. Green, *Generation of the (J,H,T) Surface for Commercial Superconductor using Reduced-State Parameters* (Lawrence Berkeley Laboratory, University of California, SSC-N-502, LBL-24875, 1988).